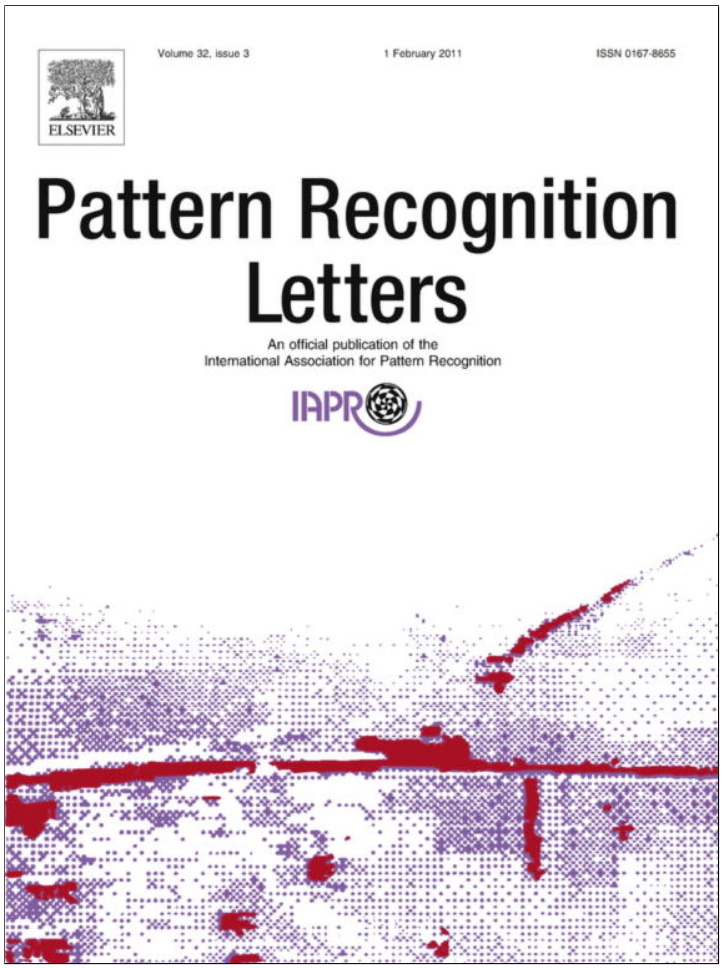

Pattern Recognition Letters 32 (2011) 524–531

Contents lists available at ScienceDirect

Pattern Recognition Letters

journal homepage: www.elsevier.com/locate/patrec

A 2-point algorithm for 3D reconstruction of horizontal lines from a single omni-directional image

Wang Chen [a], Irene Cheng [b], Zihui Xiong [a,b], Anup Basu [b,*], Maojun Zhang [a]

[a] College of Information System and Management, National University of Defense Technology, Changsha, China
[b] University of Alberta, Edmonton, Canada AB T6G 2E8

ARTICLE INFO

Article history:
Received 21 February 2010
Available online 13 November 2010
Communicated by Y. Liu

Keywords:
3D reconstruction
Horizontal line
Omni-directional image
Non-SVP imaging sensor

ABSTRACT

Reconstruction of 3D scenes with abundant straight line features has many applications in computer vision and robot navigation. Most approaches to this problem involve stereo techniques, in which a solution to the correspondence problem between at least two different images is required. In contrast, 3D reconstruction of straight horizontal lines from a single 2D omni-directional image is studied in this paper. The authors show that, for symmetric non-central catadioptric systems, a 3D horizontal line can be estimated using only two points extracted from a single image of the line. One of the two points is the symmetry point of the image curve of horizontal line, and the other is a generic point on the image curve. This paper improves on several prior works, including horizontal line detection in omni-directional image and line reconstruction from four viewing rays, but is simpler than those methods while being more robust. We evaluate how the precision of feature point extraction can affect line reconstruction accuracy, and discuss preliminary experimental results.

1. Introduction

The reconstruction of 3D scenes with abundant straight line features such as outdoor street blocks and indoor structural features has wide applications in computer vision and robot navigation. Significant effort has been devoted to the development of two-view or multi-view approaches allowing for high accuracy and complete modeling of the scenes (Hirschmuller, 2008; Leung et al., 2008; Kolmogorov, 2004; Klaus et al., 2006), based on solving the correspondence problem between two or more images. In contrast to these traditional approaches, this paper studies 3D reconstruction of straight lines from only a single 2D image, which is acquired by a symmetric non-central catadioptric camera. The correspondence problem between different images can therefore be avoided.

In general, reconstruction from a single image is a challenging and ill-posed problem. When using a perspective camera, the image of an arbitrary straight line has infinite interpretations. In fact, any straight line appearing on the viewing surface (the union set of the viewing rays associated to the line image) could have produced the line image (Caglioti et al., 2007b). In this paper, we utilize a non-central catadioptric camera (Geyer and Daniilidis, 2001), instead of classical central catadioptric cameras like those derived by Baker and Nayar (1999), to capture an omni-directional image. A non-central catadioptric system is a more general class of cameras whose viewing rays are not all concurrent, and thus can be exploited as a multi-viewpoint system to make reconstruction from a single image possible.

Several innovative approaches to analyzing straight lines in panoramic images have been proposed. A classical method in (Teller and Hohmeyer, 1999) employs four given viewing rays to compute lines which intersect the viewing rays in 3D space. Sturm (2000), Hassner and Basri (2006) present an approach to reconstruct objects from a single panoramic image, by utilizing constraints such as user-provided co-planarity, perpendicularity and parallelism. Caglioti and Gasparini (2005) study the conditions under which straight lines in 3D space can be reconstructed from single images taken by a non-central symmetric catadioptric camera. Furthermore, Caglioti et al. (2007a) relaxed the symmetry constraint, and derived geometric constraints for line localization with off-axis catadioptric cameras based on a conic mirror. With a spherical catadioptric system, Lanman et al. (2006) proposed a more general approach for line reconstruction from four image points, based on computing the Singular Value Decomposition (SVD) of the Plücker coordinates matrix of four corresponding viewing rays. Pinciroli et al. (2005) proposed an algorithm that is robust to noise and is able to retrieve 3D information of horizontal lines from a single omni-directional image, by adopting the "four viewing ray reconstruction" algorithm and RANSAC technique. Fiala and Basu (2002, 2005) used a modified Hough transform to

* Corresponding author. Tel.: +1 780 492 3330; fax: +1 780 492 1071.
E-mail addresses: chenwang@nudt.edu.cn (W. Chen), locheng@ualberta.ca (I. Cheng), xzhnudt@nudt.edu.cn (Z. Xiong), basu@ualberta.ca (A. Basu), maojun.z@gmail.com (M. Zhang).

0167-8655/$ - see front matter © 2010 Elsevier B.V. All rights reserved.
doi:10.1016/j.patrec.2010.11.011

detect horizontal lines in panoramic non-SVP images and track them as landmarks for robot navigation.

Our work is an extension to these prior techniques, mainly close to (Pinciroli et al., 2005; Fiala and Basu, 2002, 2005), which also focused on the problem of horizontal line reconstruction and detection, from a single omni-directional image. However, our novelty lies in that the equation of a 3D horizontal line can be estimated using only two points (one of them is the symmetry point of the image curve of horizontal line) extracted from a single image, rather than four points that is required in (Teller and Hohmeyer, 1999; Caglioti and Gasparini, 2005; Pinciroli et al., 2005; Swaminathan et al., 2008). We also evaluate how precision of the extracted feature points can affect line reconstruction accuracy. Preliminary experiments show that the proposed method is simpler than other approaches, while being more robust.

The remainder of this paper is organized as follows: Section 2 gives some background on horizontal line reconstruction from panoramic images. Specifics of the reconstruction using only two points are discussed in Section 3. Experimental results are presented in Section 4, following which concluding remarks are given in Section 5.

2. Horizontal line reconstruction

Straight lines often constitute the majority of structural features in urban scenes. An example is shown in Fig. 1, where Fig. 1a is an omni-directional image captured with a catadioptric camera in a housing complex, and Fig. 1b is the corresponding unwrapped panorama in which edges of buildings and enclosures, even grid-lines on the ground, generate features corresponding to horizontal (parallel to the ground plane) lines. Although it is hard to ensure theoretical horizontality of these lines for most scenes, it is rational to make this "horizontal" assumption since horizontality is a basic principle of architecture, especially for urban and indoor environments. A similar assumption is also implicitly made in (Pinciroli et al., 2005; Fiala and Basu, 2002, 2005).

The image sensor used in this paper is a non-central parabolic catadioptric camera, as illustrated in Fig. 2. The sensor is placed perpendicular to the ground with an assistant gradienter (an equipment that can be used to measure the gradient and horizontality), to make the image plane of a camera parallel to the ground. In this section, we review the imaging formation of a catadioptric system for analyzing the property of horizontal line images. Fig. 3 shows the XZ section of the imaging model.

In Fig. 3, O denotes the origin of the coordinate system, $P_1 = (x_1, z_1)$ is a point in space, $m_1 = (x_{m1}, z_{m1})$ and $p_1 = (-R_1, 0)$ are the incidence point and image point of P_1 respectively, f is the camera focal length, and the equation of the mirror section is $z = kx^2$. Following the laws of reflection, we have:

$$\tan\alpha_1 = 2kx_{m1}, \quad \tan\beta_1 = \frac{f}{R_1}, \quad \tan\theta_1 = \frac{z_1 - z_{m1}}{x_1 - x_{m1}},$$

and

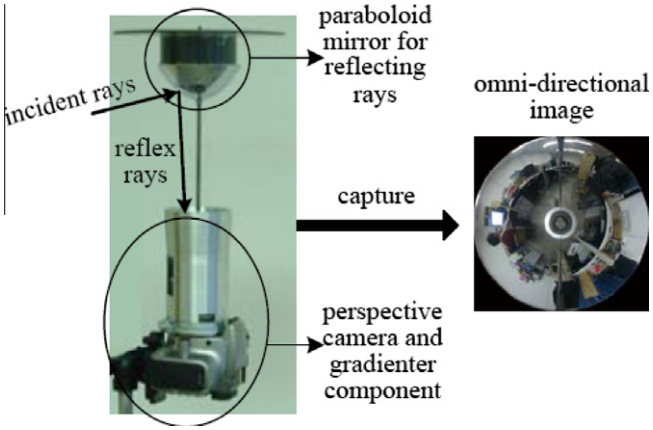

Fig. 2. Non-central parabolic catadioptric camera.

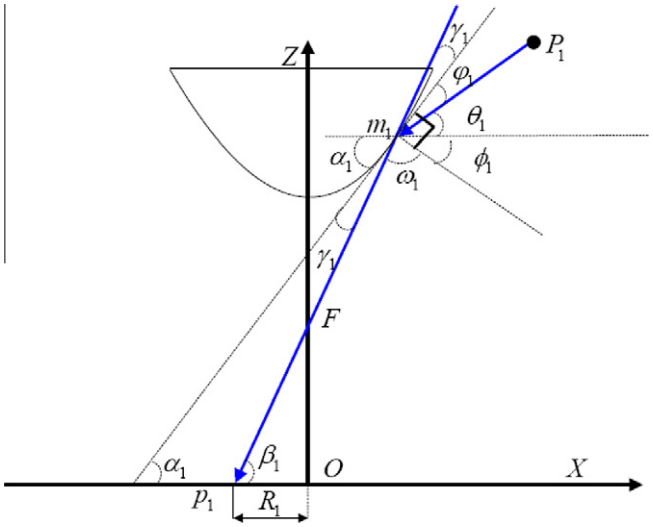

Fig. 3. XZ section of the imaging model.

$$\begin{cases} \beta_1 = \theta_1 + \varphi_1 + \gamma_1 \\ \alpha_1 = \theta_1 + \varphi_1 \\ \theta_1 + \varphi_1 + \phi_1 = 90^\circ \\ \omega_1 + \gamma_1 = 90^\circ \\ \theta_1 + \varphi_1 = \omega_1 \end{cases} \Rightarrow \begin{cases} \beta_1 = \theta_1 + \varphi_1 + \gamma_1 \\ \alpha_1 = \theta_1 + \varphi_1 \\ \varphi_1 = \gamma_1 \end{cases} \Rightarrow \theta_1 = 2\alpha_1 - \beta_1 \tag{1}$$

Similarly, suppose $P_2 = (x_2, z_2)$ is another 3D point and $z_1 = z_2$, $m_2 = (x_{m2}, y_{m2})$ is the incidence point of P_2, $p_2 = (-R_2, 0)$ is the corresponding image point of P_2, as illustrated in Fig. 4. Given $R_2 < R_1$, we have:

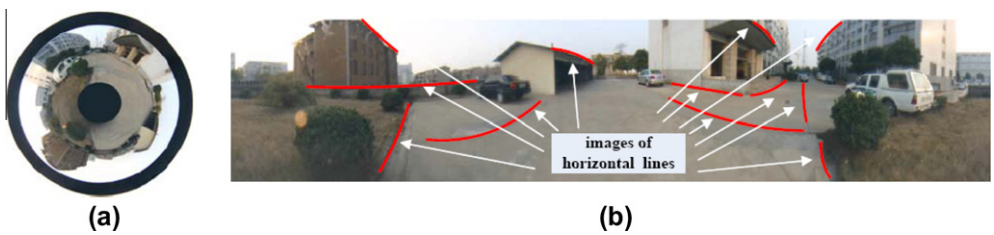

Fig. 1. Omni-directional image of an outdoor scene: (a) an omni-directional image of a housing complex; and (b) the corresponding unwrapped panoramic image.

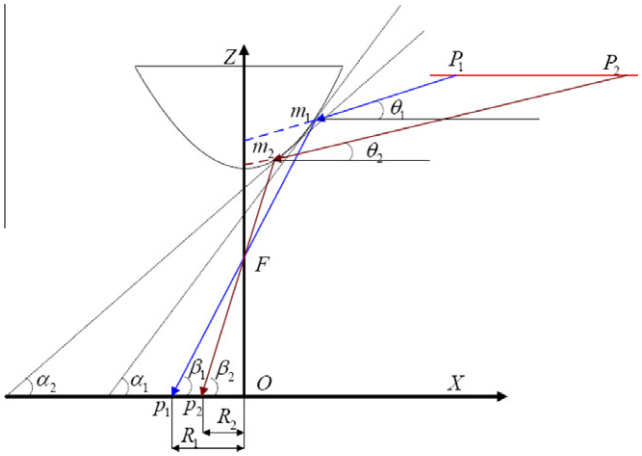

Fig. 4. Image of points with different distances to the camera axis.

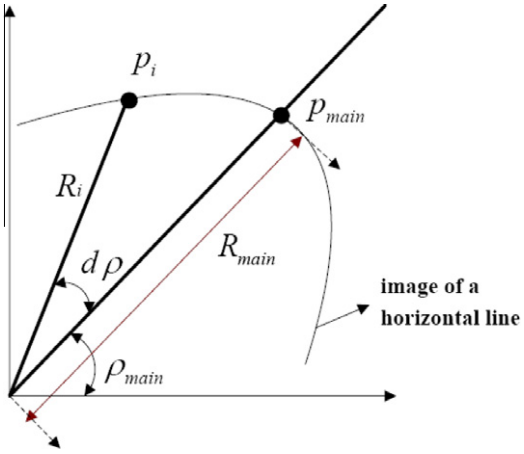

Fig. 5. Image of a horizontal line.

$$\begin{cases} \theta_2 = 2\alpha_2 - \beta_2 \\ \beta_1 < \beta_2 \\ x_{m1} > x_{m2} \\ y_{m1} > y_{m2} \\ \alpha_1 > \alpha_2 \end{cases} \Rightarrow \begin{cases} \theta_1 > \theta_2 \\ x_{m1} > x_{m2}\,, \\ y_{m1} > y_{m2} \end{cases} \text{with } z_1 = z_2 \Rightarrow \begin{cases} x_1 < x_2,\ (\theta_1 > 0, \theta_2 > 0) \\ x_1 > x_2,\ (\theta_1 < 0, \theta_2 < 0) \end{cases} \tag{2}$$

Eq. (2) indicates that, for 3D points with the same Z coordinates and satisfying $\theta > 0$, the farther the point is away from the axis of image sensor (Z axis), the closer is its image point to the image center. That is, for pixels corresponding to a 3D horizontal line, the distance between a pixel and the image center decreases depending on the distance of the corresponding 3D point from the camera axis. Similarly, when $\theta < 0$, an inverse conclusion can be deduced, i.e., the distance between a pixel and the image center increases depending on the distance of the corresponding 3D point to the camera axis. While $\theta = 0$ is a degenerate case that has been discussed in (Caglioti and Gasparini, 2005). Especially, if two pixels have the same distances to the image center, they must be symmetric to the radial line that contains the image of the 3D point which has the shortest distance to the camera axis. This property of horizontal line images can be used to simplify the detection of horizontal lines from a single omni-directional image, e.g., to exclude image curves that do not satisfy this property, since they do not necessarily correspond to 3D horizontal lines. For example, assume L is a non-horizontal line, ℓ is the image curve of L, O is the image center, p_m is the image of the specific point that has the shortest distance to the camera axis, and p_i and p_j are two different pixels on ℓ, then, if p_i and p_j are symmetric to $p_m O$, we have $|\vec{p_i O}| \neq |\vec{p_j O}|$; on the other hand, if $|\vec{p_i O}| = |\vec{p_j O}|$, the pixels p_i and p_j cannot be symmetric to $p_m O$.

Given the above relationship between points on 3D horizontal lines and their images, how does the entire image of a horizontal line look like? As discussed in (Fiala and Basu, 2002, 2005), for a general non-SVP catadioptric system, a 3D horizontal line projects to a complex non-circular curve which can be defined by ρ_{main} and R_{main}, and projections of all points on the line are then represented by R_i and $\rho_{main} + d\rho$, as illustrated in Fig. 5, where $p_{main} = (R_{main}, \rho_{main})$, $p_i = (R_i, \rho_i) = (R_i, \rho_{main} + d\rho)$ are pixels in polar coordinates, and p_{main} is the image of the point on the horizontal line that is closest to the camera axis. For the completeness and clarity of following discussion, here we give a formal definition of p_{main} as:

Definition 1. With a non-SVP omni-directional catadioptric camera, assume O is the image center, ℓ is the image curve of a horizontal line L, then the main-point p_{main} of ℓ is the point that satisfies:

$$\text{For } \forall p_i, q_j \in \ell, (p_i \text{ and } q_j \text{ are symmetric to } \vec{p_m O}) \iff (|\vec{p_i O}| = |\vec{p_j O}|)$$

Given the image curve ℓ, it is easy to extract p_{main} according to Definition 1, since we can compute the distances of $|\vec{p_i O}|$ for all $p_i \in \ell$ clockwise and then find the distance inflexion point as the p_{main}.

In the following discussion, we focus on the problem of line reconstruction and we assume that the image curves of horizontal lines have been extracted, and all image points are in the form (R, ρ). (Please refer to the literature on horizontal line detection from a single omni-directional image for details (Fiala and Basu, 2002, 2005.)

3. Horizontal line reconstruction from two points

In this section, we first review the analytic mapping from image points to 3D rays for a parabolic catadioptric system, and then propose our reconstruction algorithm.

3.1. 3D ray from an image point

To get the 3D ray from an image point, we consider the ray traveling in the opposite direction, from image plane through the pinhole to 3D space after being reflected off a parabolic mirror, as illustrated in Fig. 6.

Here O denotes the origin of the coordinate system, $p_i = (R_i, \rho_i)$ is a point on the image curve of a horizontal line, $m_i = (x_{mi}, y_{mi}, z_{mi})$ is the incidence point, $O'F = L$ is the distance between pinhole F and the vertex O', $FO = f$ is the focal length of the camera, and the mirror equation is $z = k(x^2 + y^2) + f + L$. Note that m_i can be solved by computing the intersection point of $\vec{p_i m_i}$ and the parabolic mirror.

$$\begin{cases} z_{mi} = k(x_{mi}^2 + y_{mi}^2) + f + L \\ \frac{x - x_{mi}}{R_i \cos(\rho_i) - x_{mi}} = \frac{y - y_{mi}}{R_i \sin(\rho_i) - z_{mi}} = \frac{z - z_{mi}}{z_{mi}} \end{cases} \tag{3}$$

While u_i, as the unit vector of the corresponding reflected ray of p_i, can also be determined based on Eq. (1) to obtain:

$$u_i = (\cos(\rho_i)\cos(\theta_i), \sin(\rho_i)\cos(\theta_i), \sin(\theta_i)) \tag{4}$$

Where

$$\begin{cases} \theta_i = 2\alpha_i - \beta_i \\ \tan\alpha_i = 2k\sqrt{(x_{mi}^2 + y_{mi}^2)} \\ \tan\beta_i = f/R_i \end{cases}$$

Thus, a 3D reflected ray t_i, corresponding to p_i, can be written as:

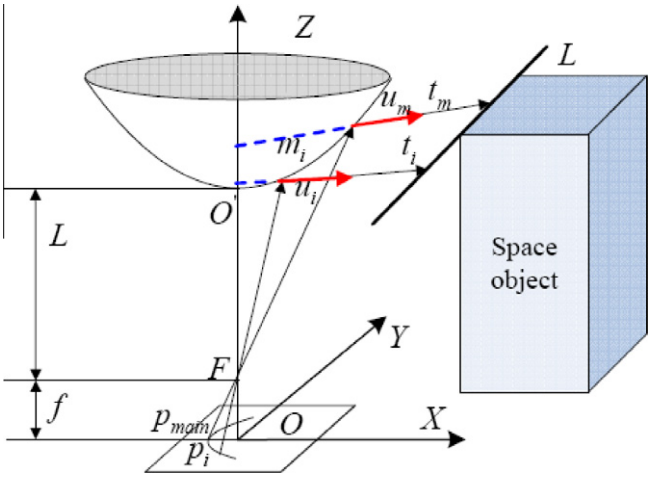

Fig. 6. Horizontal line from two viewing rays reflected off a parabolic mirror.

$$t_i = m_i + \lambda u_i \tag{5}$$

3.2. Determining a horizontal line from two rays

In a non-SVP parabolic catadioptric camera, not all reflected rays intersect the axis at the same point as shown in Fig. 6. In fact, for two image points that are not congruent modulo a rotation around the optical axis, their corresponding reflected rays are twisted, i.e., the two rays are not coplanar. This property makes reconstruction of a 3D line from a single image possible.

All present algorithms in this field require four viewing rays, i.e., four corresponding points on the image curve of a horizontal line, to reconstruct the line by computing lines intersecting the four given viewing rays. This is because in general, there are an infinite number of lines intersecting three or less lines in 3D space, exactly two lines intersecting four given lines, and none intersecting more than four lines (Teller and Hohmeyer, 1999). However, we found that for image curves of a horizontal line defined by ρ_{main} and R_{main} (Fiala and Basu, 2002, 2005), it is possible to reconstruct the line from only two points on the curve: one is $p_{main} = (R_{main}, \rho_{main})$, and the other is an arbitrary point $p_i = (R_i, \rho_i)$, $0 < |\rho_i - \rho_{main}| < 90°$, as shown in Fig. 6. From these two viewing rays corresponding to the two given points, exactly one horizontal line can be determined. In fact, we can prove the following theorem:

Theorem 1. *With a calibrated non-SVP omni-directional catadioptric camera, given two image points $p_{main} = (R_{main}, \rho_{main})$ and $p_i = (R_i, \rho_i)$, $0 < |\rho_i - \rho_{main}| < 90°$ of a horizontal line L, L can be uniquely determined.*

Proof. Since the imaging sensor is calibrated, and p_{main}, p_i are given, according to Section 3.1 and Fig. 6, the viewing rays t_m and t_i corresponding to p_{main} and p_i can be estimated. Therefore, there are four independent constraints on L:

(1) $L \perp t_m$: t_m is the corresponding viewing ray of p_{main}, and p_{main} is the image of the closest point on L to the camera axis, hence L is perpendicular to the plane formed by t_m and the camera axis. Consequently, $L \perp t_m$.
(2) L intersects t_m: t_m is the corresponding viewing ray of p_{main}, and p_{main} is the image of a point on L, thus L must intersect t_m at some point.
(3) L intersects t_i: t_i is the corresponding viewing ray of p_i, and p_i is the image of a point on L, thus L must intersect t_i at some point.
(4) L is horizontal: this is the premise of the algorithm.

The above constraints are enough to uniquely determine the equation of L. □

We solve for L by exploiting Plücker coordinates, since it provides a convenient representation for directed lines in 3D space. If a and b are two directed lines, and Π_a, Π_b their corresponding Plücker coordinates, a relation $side(a, b)$ can be defined as the permuted inner product:

$$side(a, b) = \Pi_a \cdot \Pi_b \tag{6}$$

which is zero whenever a and b intersect or are parallel, and non-zero otherwise (Teller and Hohmeyer, 1999).

To reconstruct the horizontal line L from t_m and t_i, we define L by setting its Z coordinates as z_L. Since $L \perp t_m$ and L intersects t_m, L can be represented as a function of one parameter z_L. According to Eq. (6), we then have $side(t_i, L) = \Pi_{t_i} \cdot \Pi_L = 0$ because L intersects t_i, from which z_L can be determined. Consequently, the horizontal line L can be determined.

Although the proposed algorithm is very simple, being an improvement on prior research, it makes full use of the characteristics of a horizontal line image, and exploits a different way to reconstruct horizontal lines from a single omni-directional image.

Additionally, notice that, the line reconstruction algorithm in this section is only determined by the two viewing rays corresponding to the two extracted image points, and has no direct link to the shape of the reflective mirror. Therefore, the proposed method can be suitable for any omni-directional catadioptric imaging sensor, given that it is symmetric around the camera axis, and the mirror is convex.

4. Experimental results

As discussed above, 3D horizontal lines can be reconstructed from either four viewing rays (Teller and Hohmeyer, 1999; Lanman et al., 2006; Pinciroli et al., 2005), or two viewing rays as proposed in this paper. Since these rays are all derived from image points of a horizontal line, the accuracy of reconstruction naturally depends on the accuracy of image point extraction and camera calibration. Lanman et al. (2006) evaluated the calibration accuracy necessary for reconstruction from a single image, and studied the effect of calibration errors on reconstruction. In this section, we focus on the sensitivity of our algorithm to extraction precision of image points, via simulation, and compare it with the classical reconstruction algorithm which utilizes four viewing rays (Lanman et al., 2006).

4.1. Reconstruction under different extraction precisions

Theoretically, if the coordinates of extracted image points are sufficiently precise, reconstruction from either four viewing rays or two viewing rays can both obtain good results. This is so because computing lines in 3D space that intersect given viewing rays is purely a mathematical problem, and has nothing to do with other factors. Our simulation shows that, when image points have a precision of 10^{-6} cm, the two approaches are almost comparable, and both have error rates of about 0.1%. However, precision of 10^{-6} cm is hard to achieve in practical situations, and the common precision of image point extraction varies between 10^{-3} cm and 10^{-4} cm, depending on the size of captured image and the resolution of a camera's CCD.

To evaluate the sensitivity of horizontal line reconstruction to extraction precision of image points, we use an ideal catadioptric camera model, which has the same camera parameters as our real imaging sensor shown in Fig. 2, to simulate the imaging procedure

of a 3D horizontal line. At the same time, random perturbations to image point coordinates are introduced, to make them accurate at different precision levels between 10^{-3} cm and 10^{-4} cm. After an omni-directional image is captured, four points and two points (one being $p_{main} = (R_{main}, \rho_{main})$) are randomly picked from the image curve of a horizontal line to execute the reconstruction procedures 200 times. Since reconstructed lines are supposed to be horizontal and perpendicular to t_m (the viewing ray corresponding to p_{main}, as shown in Fig. 6), we can use the distances of lines from the camera axis as the criteria to measure the reconstruction results. Fig. 7 shows the results of both the proposed method and the classical "four viewing rays reconstruction" algorithm, where the distance of a 3D line from the camera axis is set to 300 cm (as labeled in red), and the height is set to 200 cm.

Fig. 7 indicates that, the more precise the image point coordinates is, the more precisely the 3D line can be reconstructed. Under extraction precisions of 10^{-3} cm and 10^{-4} cm, the average error rates of "four viewing rays reconstruction" algorithm are about 5% and 2% respectively, while the corresponding error rates of the proposed method are about 3% and 1%. This shows that our approach is about twice as accurate as the previous method.

4.2. Reconstructing lines at different distances

To evaluate the sensitivity of reconstruction algorithms to variations in depth, we construct 3D horizontal lines at different distances from the camera axis, assuming the same precision in feature point extraction. In this experiment, the heights of 3D lines are all set to 200 cm, and the distances are set between 250 cm and 500 cm. We reconstruct lines with four and two randomly picked image points respectively, repeat the process 200 times (as in Section 4.1), and compute the mean values as the final results.

As illustrated in Fig. 8, for lines at different distances, reconstruction with the proposed method is more precise than that from four image points, under extraction precisions of both 10^{-3} cm and 10^{-4} cm. In Table 1, we give some specific comparisons between these two methods at some selected distances. Distance error rates of the reconstructed lines under extraction precision of 10^{-4} cm are shown in Fig. 9, and their corresponding orientation errors are illustrated in Fig. 10. Since in this experiment, we pick image points randomly (except the *main point*), the results obtained in Figs. 9 and 10 look somewhat fluctuating. However, one can clearly see that the distance error rate generally increases depending on

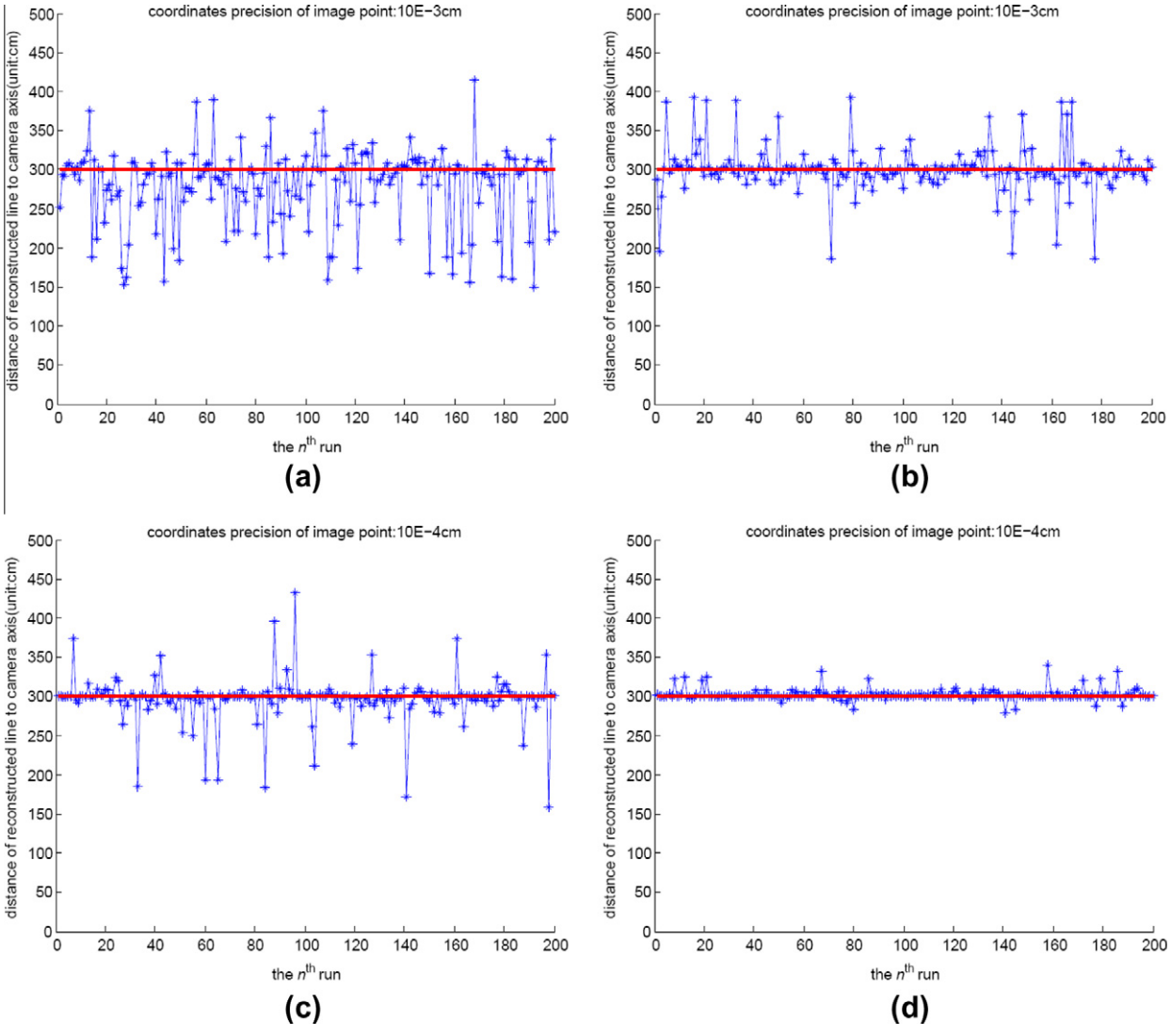

Fig. 7. Reconstructing horizontal lines under different extraction precisions (red horizontal line: ground truth; blue scattered points: reconstruction result). (a, c) reconstruction from four points; (b, d) reconstruction using the proposed method. (For interpretation of the references to colour in this figure legend, the reader is referred to the web version of this article.)

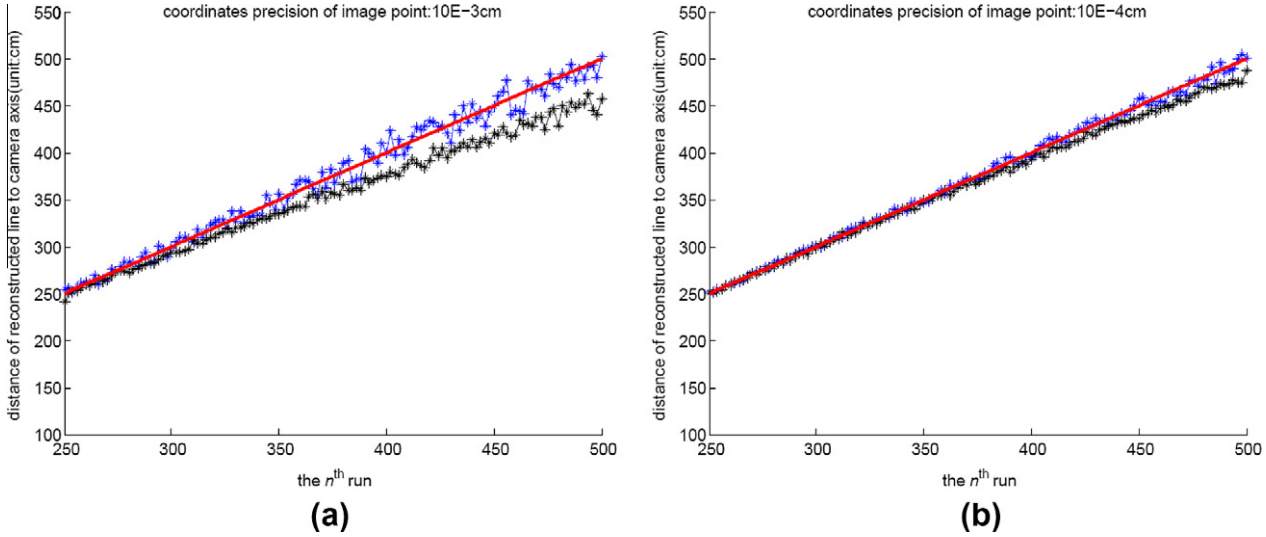

Fig. 8. Reconstructing 3D lines at different distances (red line: ground truth, black curve: reconstruction from four points; blue curve: reconstruction from two points). (a) Reconstruction under extraction precision of 10^{-3} cm; (b) reconstruction under extraction precision of 10^{-4} cm. (For interpretation of the references to colour in this figure legend, the reader is referred to the web version of this article.)

the distance of the line to the camera axis, while the orientation error, which mainly depends on the accuracy of the estimation of the *main point*, is less correlated with the line distance.

Table 1
Comparing reconstruction at specific distances (errors in parenthesis).

Distance of lines	Reconstructed distance			
	Reconstruct from four points		Reconstruct with proposed method	
	10^{-3} cm	10^{-4} cm	10^{-3} cm	10^{-4} cm
250	247.8 (2.2)	248.9 (1.1)	252.3 (2.3)	249.8 (0.2)
300	294.5 (5.5)	298.6 (1.4)	297.2 (2.8)	300.7 (0.7)
350	341.3 (8.7)	346.2 (3.8)	343.1 (6.9)	353.4 (3.4)
400	376.6 (23.4)	391.5 (8.5)	381.8 (18.2)	395.3 (4.7)
450	414.7 (35.3)	436.9 (13.1)	434.2 (15.8)	443.8 (6.2)

Figs. 8a and 9 also show that, under the extraction precision of 10^{-3} cm, acceptable reconstruction, with an average error rate of less than 5%, is possible only for lines within a distance of 450 cm. To correctly reconstruct lines beyond this distance, one effective way is to improve the accuracy of feature point extraction. However, this is difficult to achieve with algorithm improvement because it depends mainly on the image sensor precision.

4.3. Reconstruction from real omni-directional images

In this section, examples of reconstruction from real omni-directional images are presented. A two stage calibration procedure is used to obtain precise intrinsic and extrinsic camera parameters: (1) intrinsic calibration of the camera, (2) estimation of mirror pose with respect to the camera, as in (Tomohiro et al., 2006). The test images are shown in Fig. 11(a, b), which are captured with a non-central catadioptric camera (Fig. 2). Two image

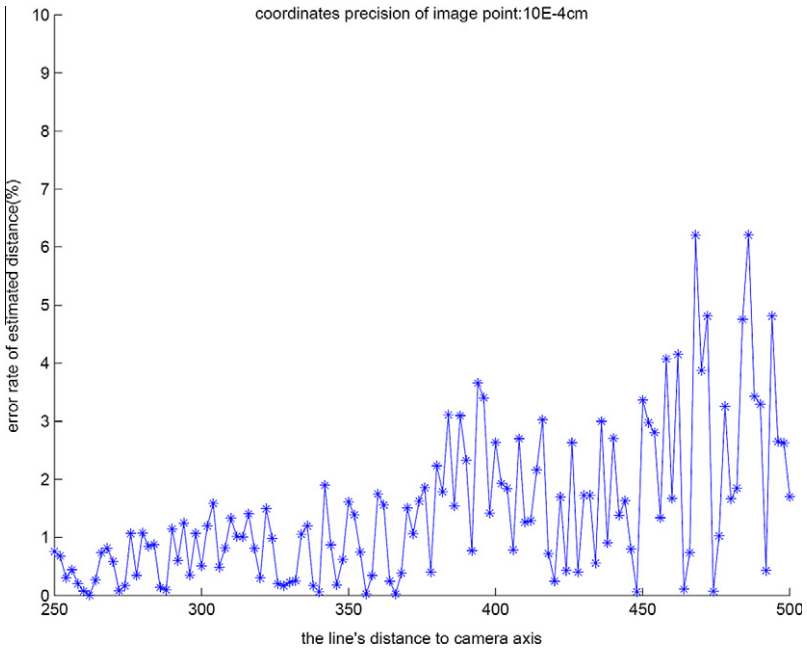

Fig. 9. Error rate of estimated distance.

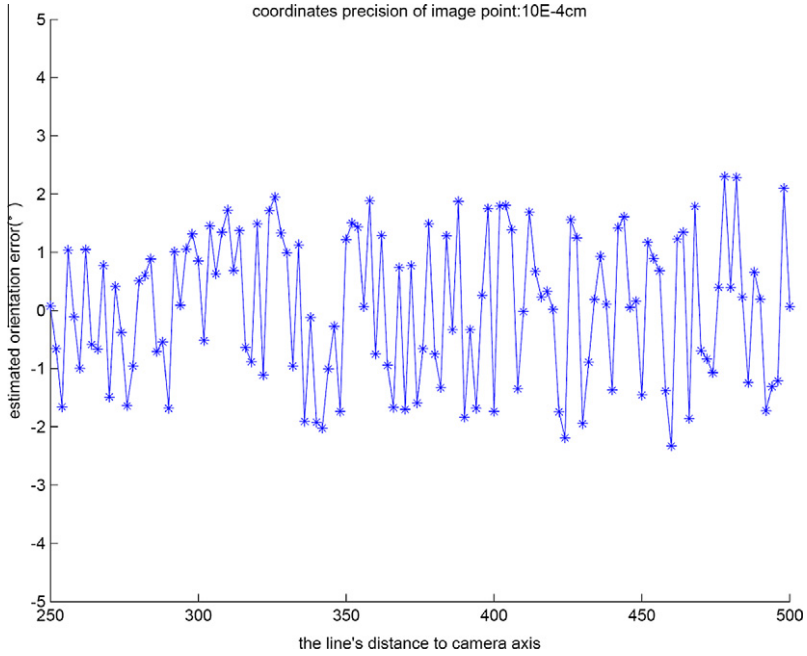

Fig. 10. Estimated orientation error.

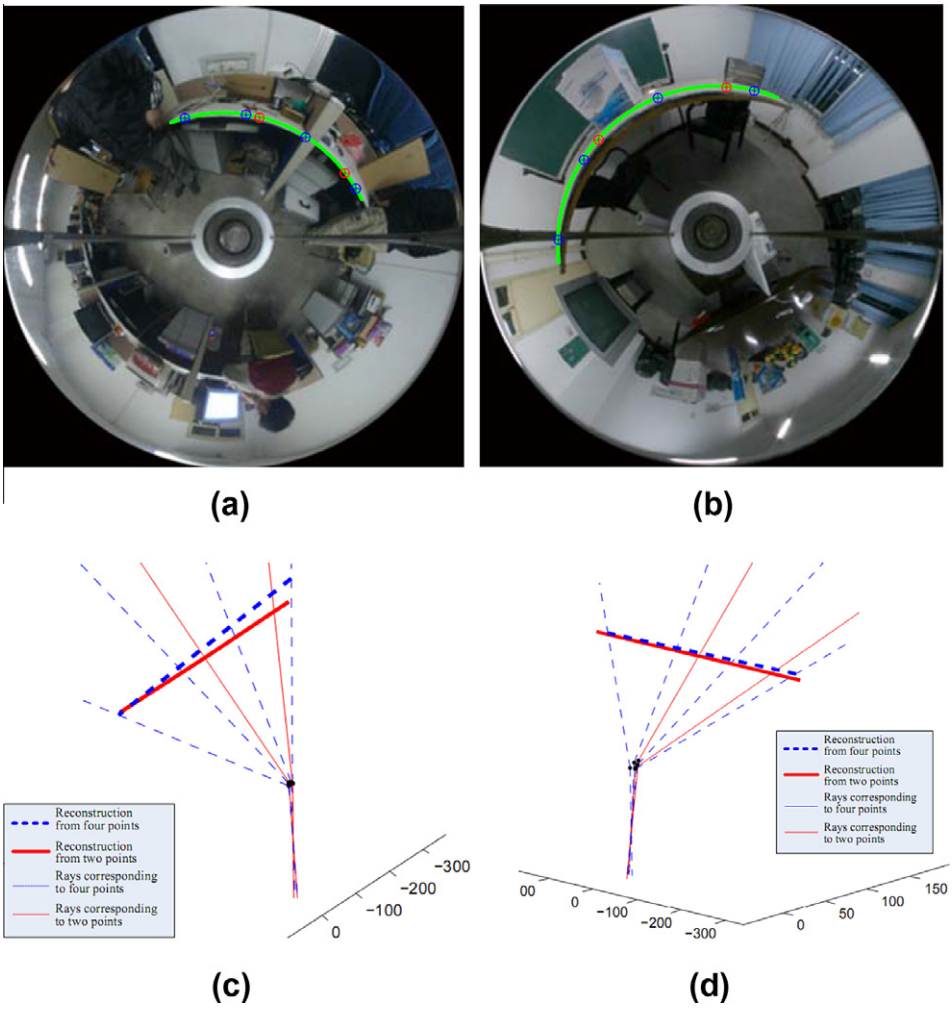

Fig. 11. Line reconstruction from real omni-directional images: (a, b) omni-directional images captured in a lab and a meeting room; (c, d) line reconstructions from (a) and (b) respectively with different methods (four image points and two image points).

curves corresponding to horizontal lines in omni-directional images are correctly detected using the method proposed in (Fiala and Basu, 2002). A sub-pixel corner detection algorithm (Bouguet, 2010) is used to refine the manually-selected image points. Following the method outlined in Sections 3, we estimate the equations of 3D horizontal lines, as illustrated in Fig. 11(c, d). Since ground truth is not available, we compare our reconstruction (shown in solid red) to that obtained using four viewing rays (shown in dotted blue). Notice that the line reconstructed with the proposed method is closer to horizontal, which supports the error observations made from simulations in Section 4.1.

5. Conclusion

In this paper, we proposed a novel approach advancing prior approaches (Pinciroli et al., 2005; Fiala and Basu, 2002) to reconstruct horizontal lines in 3D space from a single 2D omni-directional image, captured with a non-SVP catadioptric camera. Our method reconstructs a 3D horizontal line using only two points extracted from that line from a single image, rather than four points that were needed in prior works. Preliminary experiments and simulations validate the correctness of the proposed method which is simpler than previous approaches while being more robust to errors in feature point extraction.

Although our approach shows improvement over previous methods, we believe further enhancement can be obtained by addressing issues like imaging noise, and quantization error. Future studies will also focus on developing more robust image acquisition platforms and appropriate calibration methods.

References

Baker, S., Nayar, S.K., 1999. A theory of single-viewpoint catadioptric image formation. Internat. J. Comput. Vision 35 (2), 175–196.

Bouguet, J.Y., 2010. Camera calibration toolbox for matlab. <http://www.vision.caltech.edu/bouguetj>.

Caglioti, V., Gasparini, S., 2005. On the localization of straight lines in 3D space from single 2D images. In: Proc. Internat. Conf. on Computer Vision and Pattern Recognition, 1, pp. 1129–1134.

Caglioti, V., Taddei, P., Boracchi, G., Gasparini, S., 2007a. Single-image calibration of off-axis catadioptric cameras using lines. ICCV, 1–6.

Caglioti, V., Gasparini, S., Taddei, P., 2007b. Methods for space line localization from single catadioptric images new proposals and comparision. In: Proc. Internat. Conf. on Computer Vision, 14(21), pp. 1–6.

Fiala, M., Basu, A., 2002. Hough transform for feature detection in panoramic images. Pattern Recognition Lett. 23 (14), 1863–1874.

Fiala, M., Basu, A., 2005. Panoramic stereo reconstruction using non-SVP optics. Comput. Vision Image Understanding 8 (3), 363–397.

Geyer, C., Daniilidis, K., 2001. Catadioptric projective geometry. Internat. J. Comput. Vision 45 (3), 223–243.

Hassner, T., Basri, R., 2006. Example based 3D reconstruction from single 2D images. In: Proc. Conf. on Computer Vision and Pattern Recognition Workshop, 15.

Hirschmuller, H., 2008. Stereo processing by semiglobal matching and mutual information. IEEE Trans. Pattern Anal. Machine Intell. 30 (2), 328–341.

Klaus, A., Sormann, M., Karner, K., 2006. Segment-based stereo matching using belief propagation and a self-adapting dissimilarity measure. International Conference on Pattern Recognition 3, 15–18.

Kolmogorov, V., 2004. Graph Based Algorithms for Scene Reconstruction from Two or More Views. Cornell University.

Lanman, D., Wachs, M., Taubin, G., Cukierman, F., 2006. Reconstructing a 3D line from a single catadioptric image. In: Proc. Third Internat. Sym. on 3D Data Processing, Visualization, and Transmission, 14(16), pp. 89–96.

Leung, C., Appleton, B., Sun, C., 2008. Iterated dynamic programming and quadtree subregioning for fast stereo matching. Image Vision Comput. 26 (10), 1371–1383.

Pinciroli, C., Bonarini, A., Matteucci, M., 2005. Robust detection of 3D scene horizontal and vertical lines in conical catadioptric sensors. In: Proc. 6th Workshop on Omnidirectional Vision.

Sturm, P., 2000. A method for 3D reconstruction of piecewise planar objects from single panoramic images. In: Proc. IEEE Workshop on Omnidirectional Vision, pp. 119–126.

Swaminathan, R., Wu, A., Dong, H., 2008. Depth from distortions. In: Proc. 8th Workshop on Omnidirectional Vision, Camera Networks and Non-classical Cameras, pp. 1–14.

Teller, S., Hohmeyer, M., 1999. Determining the lines through four lines. J. Graphics Tools 4 (3), 11–22.

Tomohiro, M., Yoshio, I., Masahiko, Y., 2006. Calibration method for misaligned catadioptric camera. IEICE Trans. Inf. systems 89 (7), 1984–1993.